Journal of
Water & Climate Change

IWA PUBLISHING

Journal of Water and Climate Change Vol 13 No 7, 2780 doi: 10.2166/wcc.2022.115

Climate change impact on blue and green water resources distributions in the Beijiang River basin based on CORDEX projections

Chao Dai[a], Xiaosheng Qin[a,*], Feifei Dong[b] and Yanpeng Cai[c]

[a] School of Civil and Environmental Engineering, Nanyang Technological University, Singapore 639798, Singapore
[b] Department of Ecology, Jinan University, Guangzhou 511486, China
[c] Institute of Environmental and Ecological Engineering, Guangdong University of Technology, Guangzhou 510006, China
*Corresponding author. E-mail: xsqin@ntu.edu.sg

XQ, 0000-0003-3187-7561

ABSTRACT

This study assessed the potential impact of climate change on spatiotemporal distribution of blue and green water resources in the Beijiang River basin, southern China, using the SWAT hydrological model and CORDEX-EAS regional climate models (RCMs). The outputs of three RCMs (namely RMOH, RMPI and RNCC) under two emission scenarios (RCP 2.6 and RCP 8.5) were bias-corrected by using the quantile delta mapping method for the control (1975–2004), near future (2021–2050) and far future (2061–2090) periods. Driven by the corrected climate variables, future blue and green water were assessed by using the SWAT model calibrated with streamflow data. The results indicated that the green water flow in the northwest basin predicted by RMOH under RCP 2.6 would increase up to about 2.7% in 2061–2090; RNCC suggests that most of the basin would experience the most significant reduction in green water storage (over 30%) under RCP 8.5 in the far future. For blue water, the ensemble mean of three RCMs indicates a slight decreasing trend in the northern part of the basin and an increasing one in the southern part under RCP 8.5 in the far future. Our findings could help watershed managers evaluate future hydrological risks and design appropriate adaptation strategies.

Key words: blue and green water, climate change, CORDEX, quantile delta mapping, regional climate models

HIGHLIGHTS

- Impact of climate change on blue and green water resources is assessed.
- The Beijiang River basin, southern China, is used as a study case.
- SWAT model and CORDEX-EAS regional climate models are used.
- The study is helpful for water resources management under climate change.

GRAPHICAL ABSTRACT

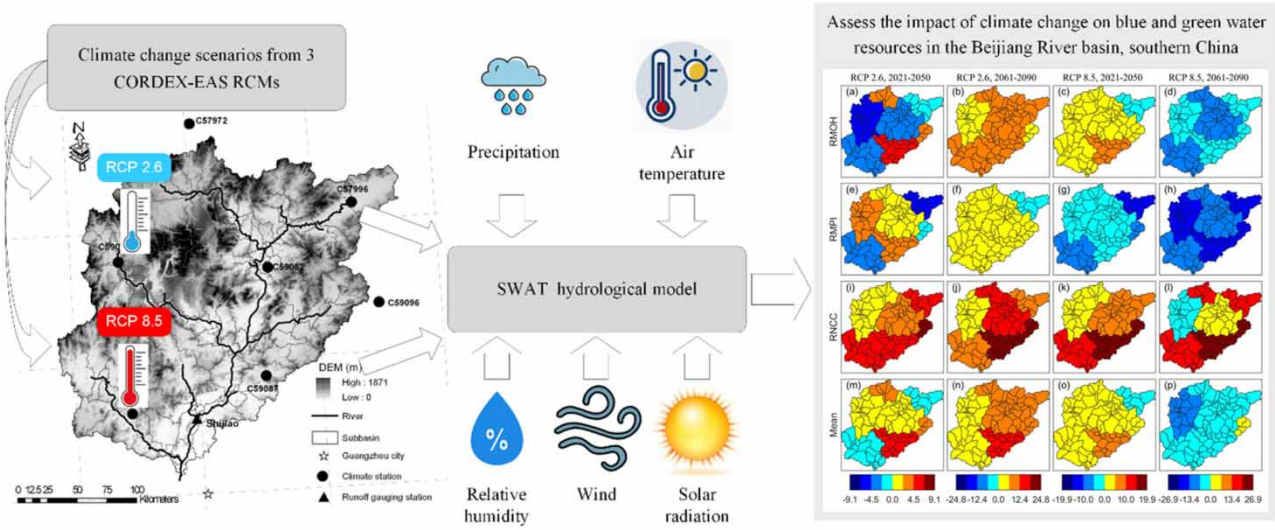

1. INTRODUCTION

Global climate change caused by the continuous rise of anthropogenic greenhouse gas emissions has had a notable impact on the hydrological cycle, subsequently affecting the regional available water resources (Hoegh-Guldberg *et al.* 2019; Padhiary *et al.* 2020). In some regions, such impacts may lead to ecological degradation and water-scarcity crisis (Zuo *et al.* 2015; Afshar *et al.* 2018). Presently, about one-third of the world's population dwells in water-scarce regions, and their lifestyles, distribution and numbers have to be changed to adapt to the water storage due to climate change (Chakilu *et al.* 2020). By 2035, the proportion of water used for energy and food will increase significantly and this will put tremendous pressure on the entire human civilization in coping with such a difficult situation (Veettil & Mishra 2016). Thus, quantification of water resources in a changing environment is important to provide guidance for adaptation strategies to achieve sustainable and efficient water use.

Previously, a large number of water resources evaluation works have explored the climate-related influences on available water resources presented as streamflow (Arnell *et al.* 2003; Islam *et al.* 2005, 2007; Gosling *et al.* 2011), lake/reservoir water storage (Sahoo *et al.* 2013) and groundwater recharge (Loáiciga *et al.* 2000). Falkenmark & Rockström (2006) opened a new angle in water management by dividing water resources into green and blue components and formalized their definitions. Green water denotes the non-runoff portion from precipitation which is deposited impermanently in the soil media and finally goes back to the atmosphere by evapotranspiration. Blue water is the part of water collected in surface or underground water bodies, like lakes, rivers and aquifers, which is utilizable directly by industry, agriculture and municipalities (Falkenmark & Rockström 2006). Obviously, the conventional water resources evaluation focusing on available water resources only considers the blue water but ignores green water. In fact, green water is also essential as it occupies over 80% of the total water resources in some arid regions and it supports the growth of crop plants and the healthy development of grassland and forest ecosystems (Schuol *et al.* 2008b; Li *et al.* 2018). Compared with the traditional evaluation method, the blue/green water concept-based climate change-related assessment is more reasonable for supporting sustainable and balanced water resources management (Rockström *et al.* 2009; Badou *et al.* 2018; Pandey *et al.* 2019; Cooper *et al.* 2022).

In general, a typical approach to appreciate future spatiotemporal changes of basin-scale blue and green water is to utilize future climate data to drive hydrological models. The Soil and Water Assessment Tool (SWAT) is a widely used sophisticated hydrological model to provide quantitative outputs of necessary water cycle components to enable computation of blue and green water distributions (Yuan *et al.* 2019a). Global circulation models (GCMs) have traditionally been utilized as the primary means for climate projections under a variety of greenhouse gas emission scenarios over long time series (Pandey *et al.* 2017). These global-scale climate projections are available from the Intergovernmental Panel on Climate Change (IPCC)'s Coupled Model Intercomparison Project (CMIP) with some experiment designs like concentration pathways (RCPs) (Taylor *et al.* 2012). Yuan *et al.* (2019b) used SWAT and five CMIP5 GCMs under the RCP 4.5 scenario to investigate the

variations of blue and green water flow/storage in the Yangtze River source region, China, for the period of 2021–2050. Farsani *et al.* (2019) assessed the spatiotemporal alterations of green and blue water amounts in the Bazoft watershed, Iran, by using SWAT and 18 emission scenarios from both CMIP3 and CMIP5 GCMs. Naderi (2020) used 22 CMIP5 GCMs to run SWAT for quantifying blue and green water amounts for the Dorudzan Dam watershed, Iran, considering climatic change influences.

It is noted that most of the above-mentioned studies have used climate data from multi-GCM ensembles to run the SWAT hydrological model to examine the climate impacts on blue and green water for a specific basin of interest. However, the recently popular CMIP5 GCMs are usually coarse (~100–300 km), and not suitable for capturing the detailed features of the basin-scale hydrological processes. Regional climate models (RCMs) are more advantageous because they produce climate variables that are more physically consistent and have higher spatial resolutions (Rummukainen 2016). The World Climate Research Programme (WCRP) Coordinated Regional Downscaling Experiment (CORDEX) initiative was launched to offer synchronized groups of regional downscaled projections for the whole world. As part of the CORDEX framework, the CORDEX-East Asia (CORDEX-EAS) initiative produces ensemble regional climate projections for East Asia, covering the study case in South China, at horizontal resolutions of around 50 km (EAS-44) and 25 km (EAS-22), based on dynamical and statistical downscaling models forced by CMIP5 GCMs. Gu *et al.* (2018b) evaluated regional climate simulations of five CORDEX-EAS RCMs and found that these RCMs could well depict the major climatological variabilities of temperature and precipitation over China. Currently, some studies have emerged to use the CORDEX-EAS RCMs for the application of climate change impact on extreme flow over the Yangtze River Basin Gu *et al.* (2018a), operational performance of reservoir network over the Poyang Lake Basin (Dong *et al.* 2019), and water and energy security for the Three Gorges Reservoir (Hu *et al.* 2020). However, research works that focus on the impact of climate change on blue and green water at a large watershed scale using high-resolution CORDEX-EAS RCM projections are still scarce.

Thus, this study aims to use CORDEX-EAS RCM projections to drive the SWAT model to evaluate future spatiotemporal alterations of blue and green water resources over the Beijiang River basin, southern China. Firstly, we calibrate the SWAT model using the observed discharge station in the lower reaches of the Beijiang River basin, and calculate the areal information of blue and green water using the hydrological outputs of SWAT at each sub-basin. Then, three CORDEX-EAS RCMs are bias-corrected to produce future climate scenarios that can be incorporated in the hydrological simulations. Lastly, the spatiotemporal changes of the blue and green water arising from climate change in various stages of the 21st century are examined.

2. MATERIALS AND METHODS

2.1. Study area

The Beijiang River basin (23 °30′–25 °42′ N, 112 °6′–114 °42′ E) is situated at the northern portion of the Pearl River basin, one of the main river basins in southern China (as shown in Figure 1). The basin's main stream (i.e. the Beijiang River) is about 468 km long, originating from Damao Mountain in Jiangxi Province, flowing through Guangzhou City and finally discharging into the South China Sea (Luo *et al.* 2008). The basin holds a drainage area over 46,700 km^2, and the highest surface elevation is about 1,871 m in the northern region (Figure 1). The Beijiang River basin is featured by a subtropical monsoon climate, where its mean annual temperature is around 20 °C and its rainfall is about 1,800 mm (Lirong & Jianyun 2012). The Beijiang River basin has rich water resources with an annual average flow over 48 billion m^3, but the water stress in this basin has to be emphasized due to the huge blue water needs for supporting agricultural, urban and industrial water utilization for Guangzhou city and the green water needs for ensuring sustainable development of the forest ecosystem covering over 3 million hectares (Wu *et al.* 2015). Moreover, as reported by Touseef *et al.* (2020), significant changes in precipitation, surface runoff and evapotranspiration might occur due to climate change, leading to changes in water resources distributions in the Upper Xijiang River basin (i.e. an adjacent basin to the Beijiang River basin). Hence, it is imperative to examine the climate change impact on specific water components in the Beijiang River basin for ensuring sustainable development in this area.

2.2. Blue and green water estimated by the hydrological model

In this work, SWAT is adopted to describe the hydrological processes and calculate the basin-scale blue and green water quantities. The model is physically based and one of the most commonly used hydrological models that can simulate the future hydro-climate changes on water resources at a regional scale (Faramarzi *et al.* 2015; Dai & Qin 2019; Zhang *et al.* 2021). Details about this model can be found in Arnold *et al.* (1998). The data needed to build SWAT consist of digital

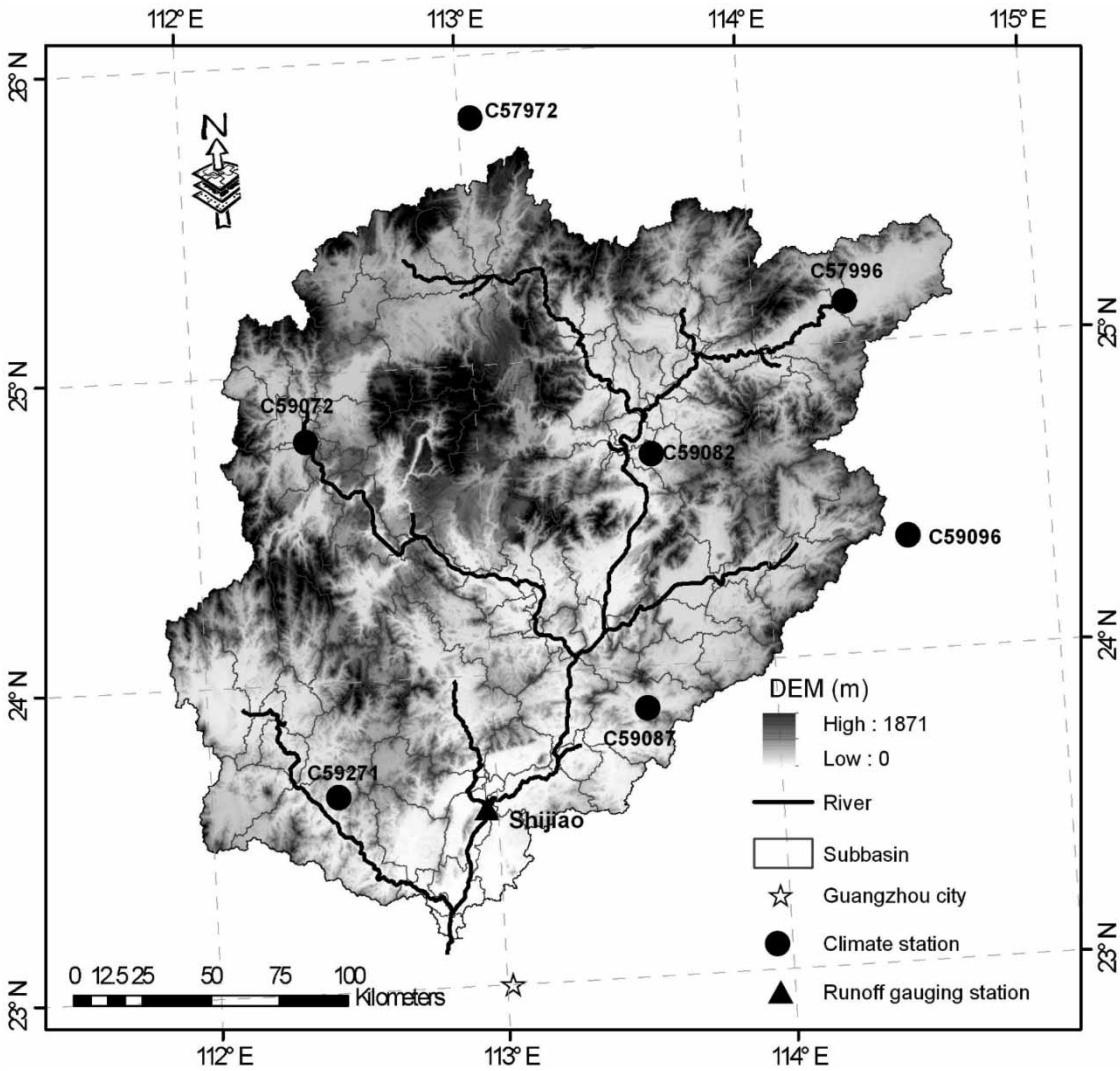

Figure 1 | Beijiang River basin map and locations of hydrometeorological stations.

elevation model (DEM), land-use and soil maps, climate and streamflow data. A 90-m resolution DEM with data range of [0, 1,871] m (Figure 1) is collected from the NASA Shuttle Radar Topographic Mission (SRTM) project (http://srtm.csi.cgiar.org). The land-use and soil map were obtained from databases of USGS Global Land Cover Characterization (GLCC; Brown *et al.* 1999) and Food and Agriculture Organization of the United Nations (FAO; Batjes 1997), respectively. The land use of the Beijiang River consisted of six main types, namely water, grassland, shrubland, forest, cropland and construction land (see Supplementary Figure S1). The two-layer soil physical property for the local SWAT soil database was estimated by the soil-plant-air-water (SPAW) tool (https://www.ars.usda.gov). The climatic data at daily scale (i.e. precipitation, air temperature, solar radiation, relative humidity and wind speed) for the period of 1975–2017 from seven stations (Figure 1 and Supplementary Table S1) were gathered from China Meteorological Data Service Center (http://data.cma.cn). The monthly streamflow data observed at the Shijiao station in the downstream of Beijiang River (Figure 1) were collected from Global Runoff Data Centre (GRDC; https://www.bafg.de) for 1981–1986 and the publications of Pan *et al.* (2017) and Li (2015) for 1987–2000 and 2001–2010, respectively.

In model processing, the Beijiang River basin was split into 105 sub-basins by using DEM and defined outlets. Each sub-basin was further disaggregated into 663 hydrologic response units (HRU) comprising specific mixtures of slope, land use and soil type. The potential evapotranspiration was computed using the FAO-56 Penman-Monteith equation (Trajkovic 2007) and surface runoff was obtained by using the soil conservation service curve number (SCS-CN) method (Mishra & Singh 2004).

The hydrological model was calibrated and validated for streamflow successively based on the runoff data at the Shijiao gauging station (Supplementary Table S2). This station was previously calibrated by Pan *et al.* (2017) and Li (2015); our study expands the time horizon to 1981–2010 and extends the research scope to include the effect of climate change on blue and green water components. In the calibration process, we used the sequential uncertainty fitting algorithm version-2 (SUFI-2) in the SWAT-CUP program (Abbaspour *et al.* 2007) to identify the optimal hydrological parameters (Table 1). Three indicators, including Nash–Sutcliffe efficiency (NSE), percent bias (PBIAS) and root-mean-square-error standard deviation ratio (RSR), are used to assess model performance (Moriasi *et al.* 2007):

$$\mathrm{NSE} = 1 - \frac{\sum_i (O_i - S_i)^2}{\sum_i (O_i - \bar{O})^2} \tag{1a}$$

$$\mathrm{PBIAS} = \frac{\sum_i (O_i - S_i)}{\sum_i O_i} \tag{1b}$$

$$\mathrm{RSR} = \frac{\sqrt{\sum_i (O_i - S_i)^2}}{\sqrt{\sum_i (O_i - \bar{O})^2}} \tag{1c}$$

where O_i and S_i are the ith observed and modelled streamflow, respectively; and $\bar{O}$ is the mean value of O_i.

After model validation, the HRU outputs of SWAT (i.e. WYLD, GW_RCHG, GW_Q, ET and SW) can provide necessary data to compute blue and green water amounts at the sub-basins (Rodrigues *et al.* 2014). The schematic diagram of blue and green water components in the SWAT model can be referred to in Supplementary Material (Zhao *et al.* 2016). The blue water is calculated by summating the water yield (WYLD) and groundwater storage. The former refers to the amount contributed

Table 1 | SWAT parameters after calibration

		Initial range		
Parameter[a]	**Calibration type[b]**	**Min**	**Max**	**Best calibrated value**
CN2	*r*	−0.2	0.5	0.237
SOL_AWC	*r*	−0.5	0.2	−0.00125
ESCO	*v*	0	1	0.172
EPCO	*v*	0	1	0.0435
SURLAG	*v*	0.1	15	6.32
OV_N	*r*	−0.2	0	−0.0301
SOL_K	*r*	−0.8	0.8	−0.607
SLSUBBSN	*r*	0	0.2	0.127
ALPHA_BF	*v*	0	1	0.399
GW_DELAY	*v*	30	450	31.5
GWQMN	*a*	−1,000	1,000	−85.0
GW_REVAP	*a*	0	0.2	0.0227
REVAPMN	*a*	1	10	1.28
CH_N2	*v*	0	0.3	0.00195
CH_K2	*v*	50	130	108
RCHRG_DP	*a*	−0.05	0.05	0.0327
ALPHA_BNK	*v*	0	1	0.182
CANMX	*v*	0	100	4.15
CH_N1	*v*	0	1	0.734

Note: [a]The detailed description and explanation of parameters can be referred to in Faramarzi *et al.* (2015).

[b]The symbols of *a*, *v* and *r* denote an absolute increase, a replacement and a relative change to the default parameter value, respectively.

from HRU through the main channel and the latter denotes the net amount between aquifer water recharge (GW_RCHG) and groundwater input to the channel (GW_Q) (Veettil & Mishra 2016). Green water could be split into two components, with one being the green water flow as equivalent to the actual evapotranspiration (ET) from the HRU, and the other one being the green water storage estimated as the soil water content (SW) (Schuol *et al.* 2008a).

2.3. Climate change scenarios and bias correction

In this study, the RCMs accustomed to drive the calibrated SWAT model are based on the CORDEX-EAS outputs downscaled from three CMIP5 GCMs. We choose the latest version of RCM originally developed by the Max Planck Institute for Meteorology and nowadays maintained by the Climate Service Center Germany (REMO2015) (Jacob 2001; Pietikäinen *et al.* 2018). The CORDEX-EAS domain REMO2015 simulation has a spatial resolution of 25 km×25 km and covers the historical range from 1951 to 2005 and the future one from 2006 to 2100. The ensemble consists of one REMO2015 RCM driven by three different GCMs, i.e. MOHC-HadGEM2-ES GCM (RMOH), MPI-M-MPI-ESM-LR (RMPI) and NCC-NorESM1-M (RNCC) (as shown in Table 2). The three RCM simulations offer climate variables required by SWAT and can be downloaded from the CORDEX-SEA website (http://www.cordex.org/domains/region-7-east-asia) at a daily time scale. We consider emission scenarios of RCP 2.6 and RCP 8.5 and use the RCMs simulations for control period (1975–2004) and projections for two future windows (near: 2021–2050; far: 2061–2090).

Although an RCM can downscale climate variables to finer resolution, its outputs also suffer from considerable systematic biases compared with observation (Ngai *et al.* 2017). We, therefore, adopt the quantile delta mapping (QDM) method to eliminate these systematic biases before using the outputs of RCMs for further analysis. Teutschbein & Seibert (2012) reviewed a few commonly used bias-correction methods and concluded that the QDM method achieved the best correction result. The QDM method is conducted to adjust the biases in the cumulative distribution function (CDF) of RCM outputs in connection with the observed distribution (Piani *et al.* 2010).

On a monthly scale, the observed and simulated precipitation data are normally fitted by gamma distributions (Volosciuk *et al.* 2017) and other variables like temperature are fitted by empirical distributions (Wilcke *et al.* 2013). Before QDM, we need to pre-process the simulated precipitation data as RCMs generally over-produce the number of wet days by including trace rainfall amounts. We set a wet-day threshold below which the precipitation data will be set to zero; this is to ensure the wet-day frequency in the RCM simulations match the observed wet-day frequency. After the wet-day frequency adjustment, the RCM climate outputs can be corrected using the QDM method represented by the following equations (Cannon *et al.* 2015; Tong *et al.* 2021):

$$x'_s = x_s + \{F^{-1}_{e,o,c}[F_{e,s,p}(x_s)] - F^{-1}_{e,s,c}[F_{e,s,p}(x_s)]\} \tag{2a}$$

$$y'_s = y_s \times \frac{F^{-1}_{g,o,c}[F_{g,s,p}(y_s;\, \alpha_s,\, \beta_s);\, \alpha_{o,c},\, \beta_{o,c}]}{F^{-1}_{g,s,c}[F_{g,s,p}(y_s;\, \alpha_s,\, \beta_s);\, \alpha_{s,c},\, \beta_{s,c}]} \tag{2b}$$

where x'_s and x_s denote the corrected and original RCM daily climate variables including temperature, radiation, humidity and wind; y'_s denotes the corrected RCM daily precipitation data; y_s denotes the data after adjusting the wet-day frequency based on the original RCM daily precipitation data; $F_{e,s,p}$ is the empirical CDF of RCM-simulated climate variables during

Table 2 | List of RCMs used in this study

Acronym[a]	RCM	Driving GCM
RMOH	REMO2015[b]	MOHC-HadGEM2-ES from Met Office Hadley Centre[c]
RMPI	REMO2015	MPI-M-MPI-ESM-LR from Max Planck Institute[d]
RNCC	REMO2015	NCC-NorESM1-M from Norwegian Climate Centre[e]

[a]RMOH, RMPI and RNCC denote that the RCM REMO2015 is driven by MOHC-HadGEM2-ES, MPI-M-MPI-ESM-LR and NCC-NorESM1-M GCM, respectively.
[b]REMO2015 RCM was originally developed at the Max Planck Institute for Meteorology, and nowadays further developed and maintained by German Institute for Climate Services (Jacob 2001).
[c]The details on MOHC-HadGEM2-ES can be found in https://www.metoffice.gov.uk/weather/climate/met-office-hadley-centre/index.
[d]The details on MPI-M-MPI-ESM-LR can be found in https://www.mpg.de/institutes.
[e]The details on NCC-NorESM1-M can be found in https://portal.enes.org/models/earthsystem-models/ncc-1.

the projection period; $F_{e,o,c}^{-1}$ and $F_{e,s,c}^{-1}$ are the inverse empirical CDF of observed and RCM-simulated climate variables during the control period, respectively; $F_{g,s,p}$ is the Gamma CDF of RCM-simulated precipitation with shape parameter α_s and scale parameters β_s during the projection period; $F_{g,o,c}^{-1}$ is the inverse Gamma CDF of observed precipitation with parameters $\alpha_{o,c}$ and $\beta_{o,c}$ during the control period; $F_{g,s,c}^{-1}$ is the inverse Gamma CDF of RCM-simulated precipitation with parameters $\alpha_{s,c}$ and $\beta_{s,c}$ during the control period.

3. RESULTS

3.1. SWAT model calibration and validation

Table 1 lists the estimated model parameters at the selected gauge stations using the SUFI-2 algorithm. The modelling period is set to 1976–2010, where the first 5 years is adopted for warming up and the periods of 1981–1998 and 1999–2010 are used for calibration and validation, respectively. Figure 2 illustrates the performance of both calibration (Figure 2(a)) and validation (Figure 2(b)). It is found that most of the simulated peaks in both calibration and validation stages for the period of 1987–2010 could match the observed ones well, but some peak flows from 1981 to 1986 during the calibration stage are somewhat underestimated. This may be because the observed streamflow data on the first day of each month from the GRDC database was approximated as the average streamflow for that month to calibrate the SWAT model. Overall, the goodness-of-fit statistics in terms of NSE, RSR and PBIAS are 0.60, 0.65 and 4.6% for the calibration stage, and 0.88, 0.39 and −3.3% for the validation stage, respectively, indicating a generally satisfactory match between observed and modelled streamflow. Thus, the calibrated SWAT model is considered acceptable for our further water resources evaluation study.

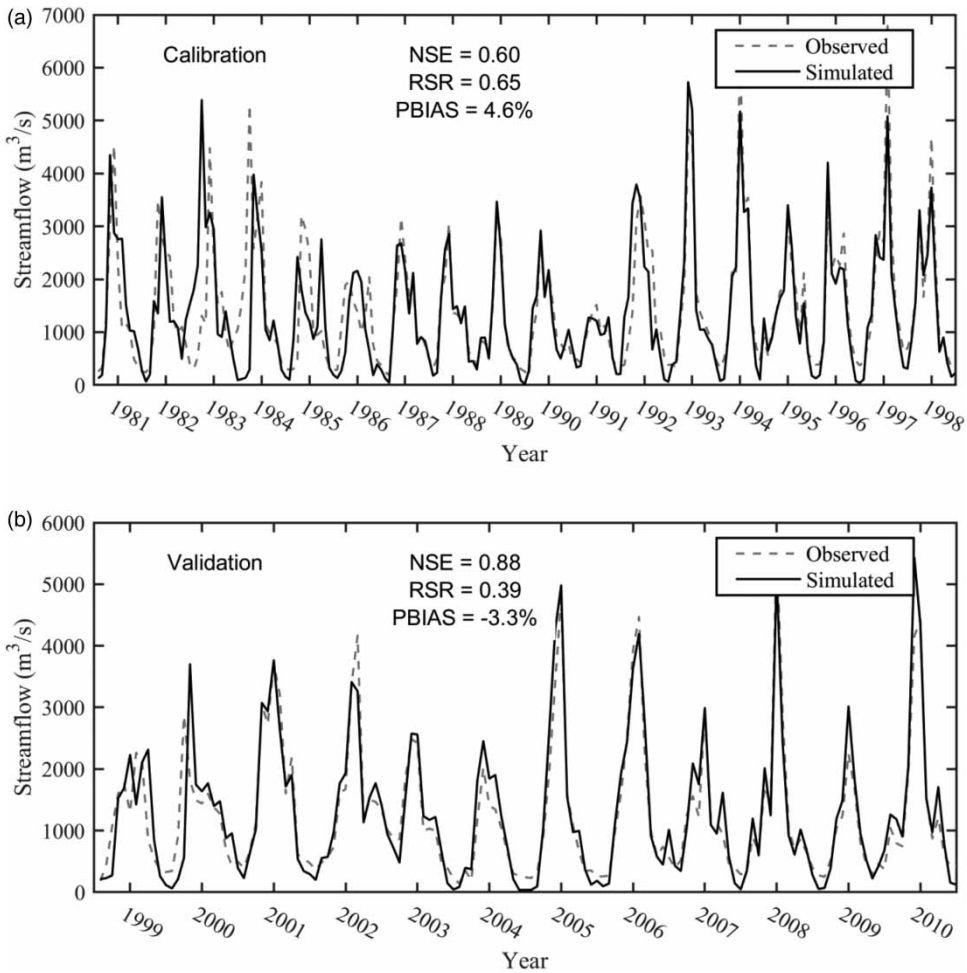

Figure 2 | Comparison between the observed and simulated monthly streamflow for (a) the calibration period from 1981 to 1998 and (b) the validation period from 1999 to 2010.

3.2. Bias correction of climate variables

The absolute bias of the monthly mean value of uncorrected and corrected RCM climate variables (i.e. precipitation, max/min temperatures, relative humidity, solar radiation and wind speed) from the monthly mean value of observed ones has been illustrated as box-whisker plots (see Supplementary Figure S3), where the box and whiskers indicate the variability of absolute bias at the seven climate stations. It is noted that the bias of climate variables before correction would vary considerably with months. In January, the absolute bias of monthly mean precipitation from uncorrected RMOH RCM would reach [0.83, 2.24] mm/day, which could be largely reduced into [−0.01, 0.15] mm/day after bias correction. In July, the absolute bias of monthly mean precipitation from uncorrected RMOH RCM would range within [−1.18, 2.91] mm/day; after bias correction, the range could be narrowed down to [−0.01, 0.26] mm/day. Figure 3 reveals the comparison results of the CDFs among the observed, uncorrected and corrected RCM-simulated climate variables at the C57972 climate station in January. Other climate stations in other months have similar results. Overall, it is revealed that (i) the CDFs of the corrected RCM-simulated climate variables are almost identical to those of the observed ones, after applying QDM and (ii) the CDFs of

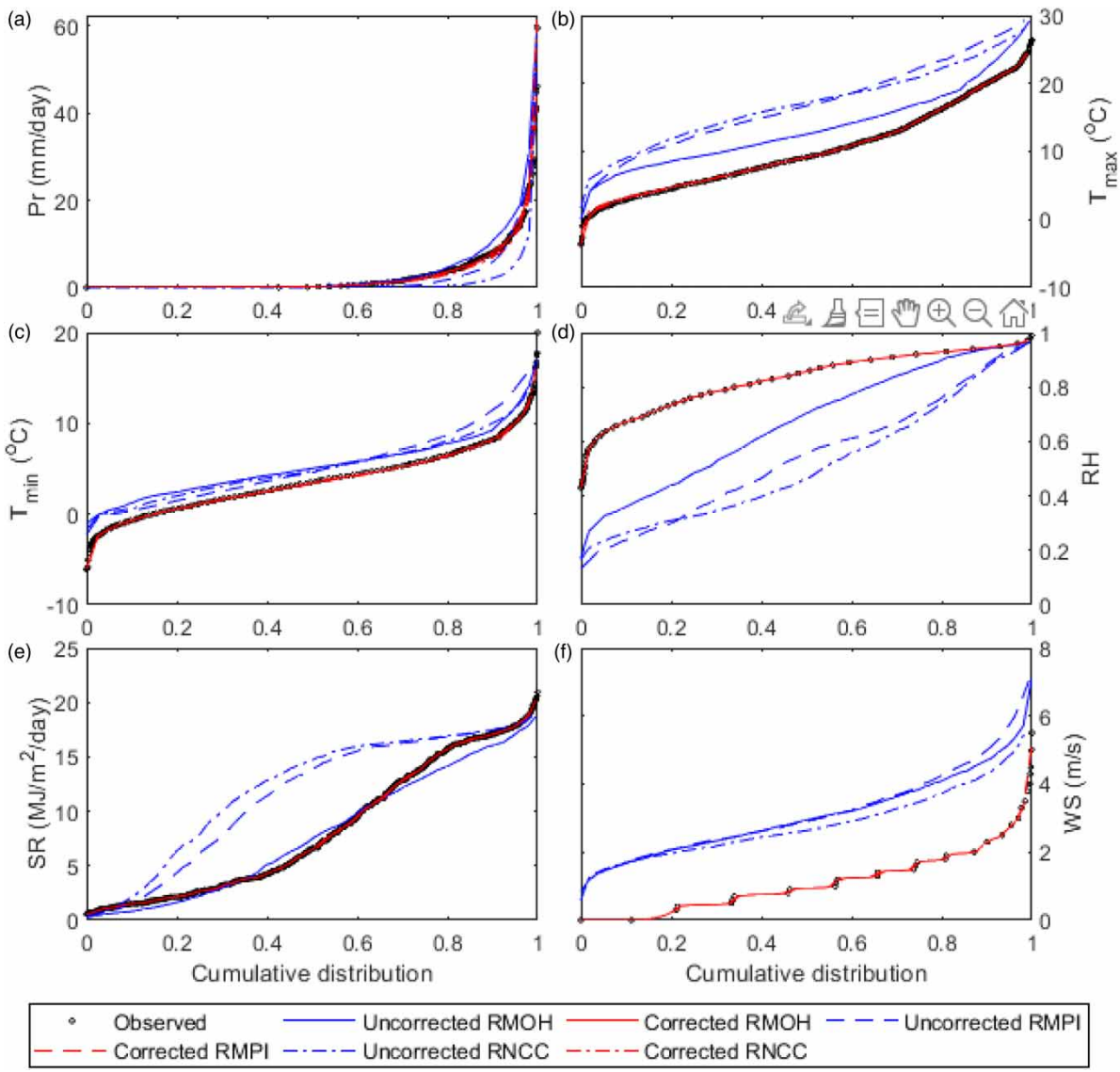

Figure 3 | Comparison of the CDFs of observed and RCM-simulated climate variables, including (a) precipitation (Pr), (b) maximum temperature (T_{max}), (c) minimum temperature (T_{min}), (d) relative humidity (RH), (e) solar radiation (SR) and (f) wind speed (WS), at the C57972 climate station for the month of January.

temperature, wind and humidity from the uncorrected RCM have significant upward and downward shifts, benchmarked with the observed data. These results imply that using the original RCM simulations to drive the SWAT model may lead to erroneous hydrologic information and bias correction is imperative for mitigating such a problem.

3.3. Availability of blue and green water during the historical period

The total annual average water resources over the Beijiang River basin from 1975 to 2004 is 1,741.46 mm, among which 33.3% (579.52 mm) is green water flow, 2.1% (36.23 mm) is green water storage, and 64.6% (1,125.71 mm) is blue water (Supplementary Table S3). Obviously, the basin was dominated by blue water in the historical period, which is about twice as much as green water. Moreover, the water balance coefficient of this basin was close to 1 for each year from 1975 to 2004 (Supplementary Table S3), implying that the components of the water cycle (i.e. precipitation, blue water, green water flow and storage) were basically in a dynamic balance. We conducted a linear regression analysis using the water cycle components during 1975–2004 (see Supplementary Figure S6), and found that (i) the precipitation and blue water are notably correlated (at a slope of 0.8705), indicating that blue water would mainly come from precipitation and (ii) the correlations of precipitation with green water flow and storage are not significant, implying that green water might primarily be affected by other factors except for precipitation (e.g. temperature, land use and cover, and soil characteristics).

Figure 4 depicts the areal information of annual means of the concerned water components based on sub-basins and historical record (i.e. 1975–2004). The annual mean precipitation ranges from 1,484 to 2,132 mm and presents a rising tendency moving from north (upstream) to southeast (downstream) (Figure 4(a)). The annual average blue water (Figure 4(d)) exhibits a spatial distribution pattern similar to that of precipitation with a range of 796–1,640 mm. The area rich in blue water resources is found in the central and southeastern portions of the basin, whereas the upstream reaches have a relatively low water yield (<900 mm). Moreover, in general, green water (Figure 4(b)) flow is more homogeneously distributed across the sub-basins than blue water flows. Higher green water flow is found mainly in the northern part of the basin (>619 mm) and lower green water flow is observed in the central and southwestern areas (<619 mm). The annual mean green water storage would decrease generally from north to south, with 48 mm being roughly the dividing magnitude (Figure 4(c)). The areal pattern of blue water is essentially in line with that of precipitation, whereas those of the other water components differ notably. This might be because precipitation predominantly affects the blue water, while the green components might be more relevant to other factors (i.e. similar reasoning from Supplementary Figure S6).

3.4. Climate change impact on precipitation, blue and green water

Precipitation is the key source in determining the magnitude of blue and green water. Figure 5 shows the basin-wide averaged annual levels of precipitation and water components during both control and future windows from the bias-corrected RCMs. It turns out that the annual precipitation (Figure 5(a)) averaged from the three RCMs is expected to slightly increase by 1.12% (from 1,645 to 1,663 mm) in the near future under RCP 2.6 and 2.48% (from 1,645 to 1,685 mm) under RCP 8.5. However, in the far future, the mean values of the three RCMs suggest a significant increase in precipitation by 7.93% (130 mm) under RCP 2.6, but a decrease by 3.90% (65 mm) under RCP 8.5, compared with control. Under RCP 2.6, the prediction trends of the three RCMs, i.e. increasing rainfall from the near to the far future, would be generally consistent. Under RCP 8.5, however, there is a significant divergence in the predictions of these RCMs, for example, RMOH predicts less rainfall from near to far future, but RNCC suggests the opposite. Moreover, from Figure 6, the spatial distributions of precipitation projected by the ensemble mean of three RCMs are somewhat consistent with the results shown in Figure 5(a). A general increasing trend is observed across the entire basin in the near future, except for a slight decrease (0.5%) in the northeast and southwest basin. Meanwhile a general decreasing trend is observed under RCP 8.5 in the far future, except for a slight increase (0.9%) in the eastern parts of the basin. Furthermore, the spatial distributions of precipitation changes from different RCMs are notably different. For example, the southwestern parts of the basin are likely to experience drier weather based on RMOH and RMPI forecasts, whereas these regions are expected to experience a wetter weather based on RNCC results.

Figures 7–9 present the relative changes of green and blue water components under RCP 2.6 and 8.5 in future windows with respect to those in the control period. The basin-scale annual averages for these water components are given in Figure 5(b)–5(d). The changes in future green water flows predicted by the RMPI indicate a relatively smaller difference between RCP 2.6 and RCP 8.5 in the near future (the average decrease level is about 3.3–4.6%), but both suggest a decreasing trend. Particularly, the green water flow projected from RMPI RCP 8.5 in basin central would decrease maximally by more than 17.9% in 2061–2090. The predicted results based on RMOH and RNCC in the near future are generally consistent with each other, but

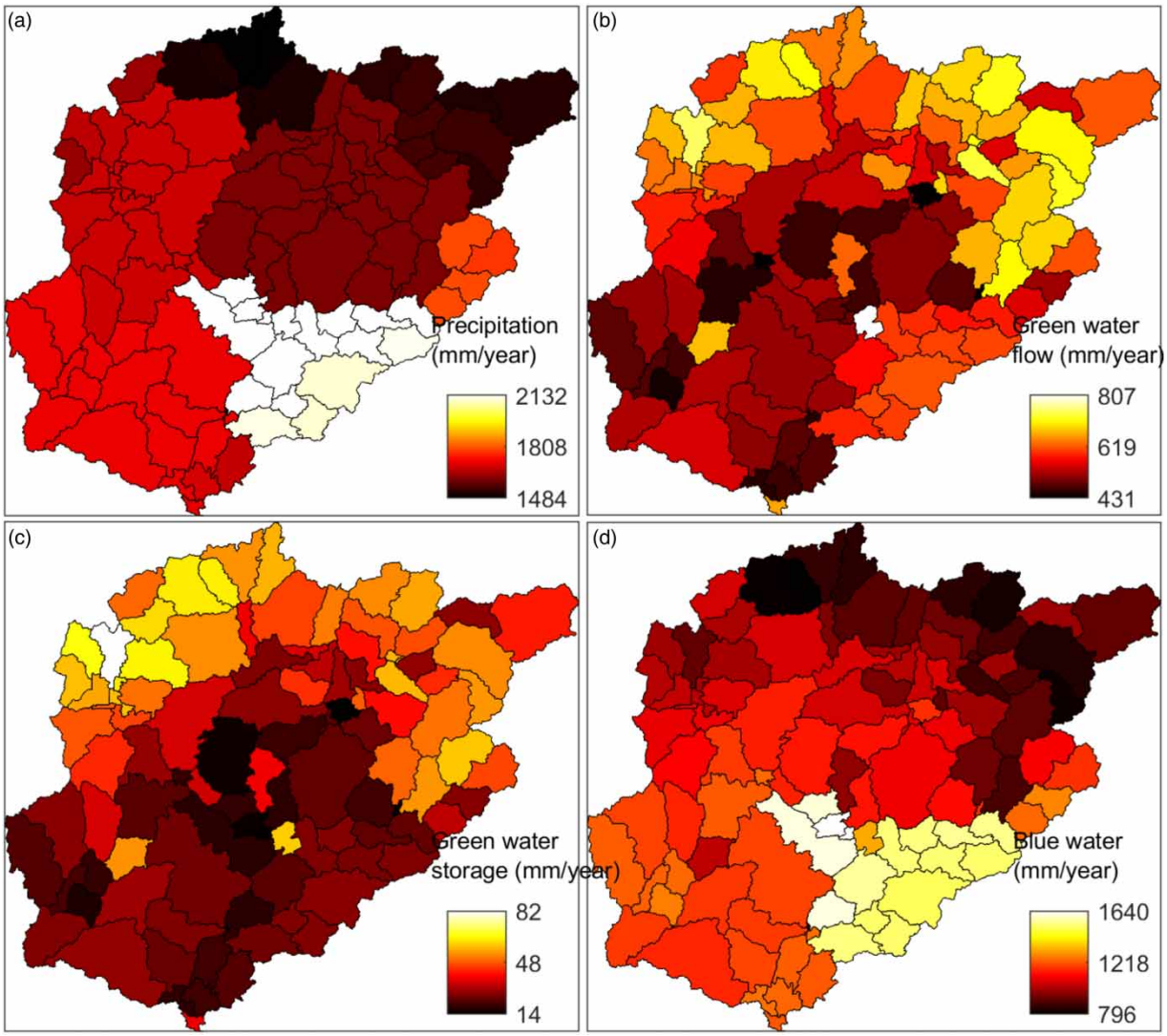

Figure 4 | Spatial distribution of annual means of (a) precipitation, (b) green water flow, (c) green water storage and (d) blue water during 1975–2004 (mm/year).

they both differ notably from the results based on RMPI. In terms of RCP 2.6, RMOH suggests an increase (~2.7%) in the northwestern part of the basin and RNCC indicates growth (~2.5%) in the southwestern part of the basin in the far future. In terms of RCP 8.5, RNCC suggests a slight increase (~1.2%) for the near future in the northern and northeast portion and RMOH also indicates a slight increase (~1.3%) over the northwestern areas. In the far future, both RNCC and RMOH suggest a minor to moderate decrease of green water flow, which is somewhat consistent with those found in RMPI. With respect to the ensemble mean of three RCMs, we find that, under RCP 2.6, the green water flow is projected to decrease by 1.5–4.6% across most areas of the basin in the near future, and only a minor decrease is suggested in the far future (except for some north and central sub-basins). Furthermore, under RCP 8.5, the green water flow is projected to decrease by 1.9–4.8% across the basin in the near future, and by 4.5–14.1% in the far future. For the overall basin (Figure 5(b)), the RCM-average green water flow is projected to decrease by 1.9% (10.5 mm) in the near future and 0.68% (3.8 mm) in the far future under RCP 2.6, and by 1.8% (10.2 mm) and 7.8% (43.3 mm) under RCP 8.5, respectively.

The spatial distribution of future green water storage changes predicted by RMOH, RMPI and RNCC appears to be relatively close, as shown in Figure 8. Under RCP 2.6 in the near future, all three RCMs suggest an overall decreasing tendency in green water storage over the basin, with RMOH forecasting a decrease up to ~19.3% in the southwestern portion, RMPI predicting a decrease up to ~12.2% in the southeastern part of the basin, and RNCC predicting a decrease up to ~18.6% in the

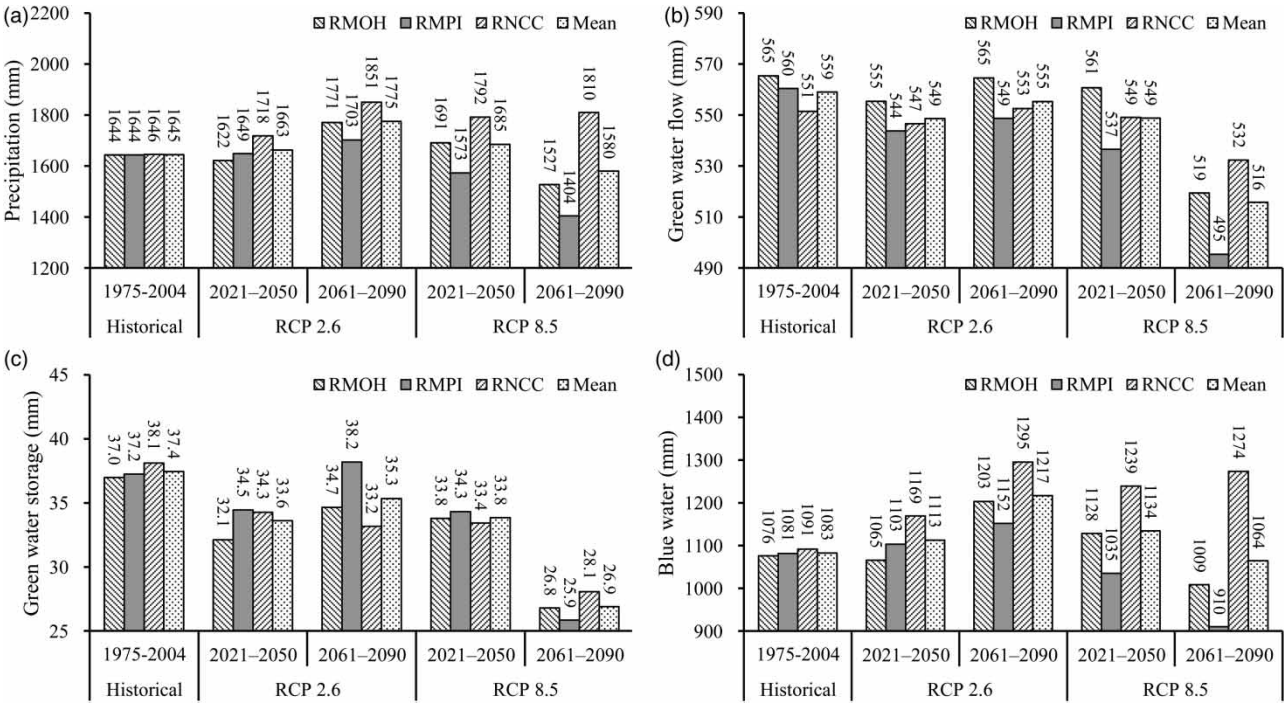

Figure 5 | Basin-scale averaged annual (a) precipitation, (b) green water flow, (c) green water storage and (d) blue water during the control period (1975–2004), near future period (2021–2050) and far future period (2061–2090) for two emission scenarios (RCP 2.6 and 8.5) from three bias-corrected RCMs.

central part of the basin. Under RCP 2.6 in the far future, RMOH and RNCC show a 7.8–31.4% reduction in green water storage in most sub-basins, while RMPI suggests a general increase over most areas of the basin with the central part of the basin having a notable increment up to 13.5%. Under RCP 8.5, the three RCMs suggest that the decreasing trend in green water storage is likely to exacerbate significantly. For example, RMOH RCP 8.5 suggests that the green water storage in the southwestern part of the basin would decrease by 16.4% in the near future and continue to decrease by up to 36.5% in the far future, whereas RMPI RCP 8.5 predicts somewhat mild decreases of green water storage (~10.1%) over the basin in the near future, and significant decreases (~38.7%) in the basin central in the far future. RNCC RCP 8.5, however, predicts a considerable decrease of green water storage in both near and far futures. In general, the green water storage is projected to decrease under most scenarios (Figure 8(m)–8(p)). Under RCP 2.6, the green water storage in the south-central part of the basin is likely to drop by 10.8–14.9% in the near future, and such a drop would become less significant (i.e. 5.8–12.4%) in the far future. Under RCP 8.5, the green water storage in the basin central area is expected to experience decreases around 11.0–16.5% in the near future, while the decrease would become more significant in the far future (i.e. 29.4–40.2%). It is worth mentioning that the basin-scale averaged green water storage, as shown in Figure 5(c), indicates a minor climate change influence on green water storage (~9.6% decrease) in the near future under both RCPs and far future under RCP 2.6, with a drastic drop (~28.1%) in the far future under RCP 8.5.

Figure 9 presents the spatiotemporal information of the simulated annual mean blue water. The basin average information can be referred to in Figure 5(d). The spatial distribution of blue water change predicted by the three RCMs under RCP 2.6 appears to be relatively consistent in the far future, but considerably different in the near term for both RCPs and far one under RCP 8.5. In the near future, RMOH RCP 2.6 predicts a considerable increase of blue water (~8.1%) near the north and southeast basin and a notable decrease (~10.6%) in the northwestern part, while RNCC predicts a general increase over the entire basin, with the eastern part of the basin having a notable rise up to 13.9%. Under RCP 2.6 in the far future, all RCMs predict an increasing tendency over the basin, whereas the RNCC predicts an increase up to 39.1% in the northern and southeastern portions of the basin. Moreover, RMPI RCP 8.5 suggests a general decreasing blue water trend over the basin. Particularly, the decreasing levels in the northeast of the basin change from 15.3 to 26.3% when the time window moves from near to far future. RMOH RCP 8.5 suggests a moderate increase (~12.4%) of blue water in the southeastern part of the basin in the near future, and a general drop (~6.5%) over the basin in the far future. Under

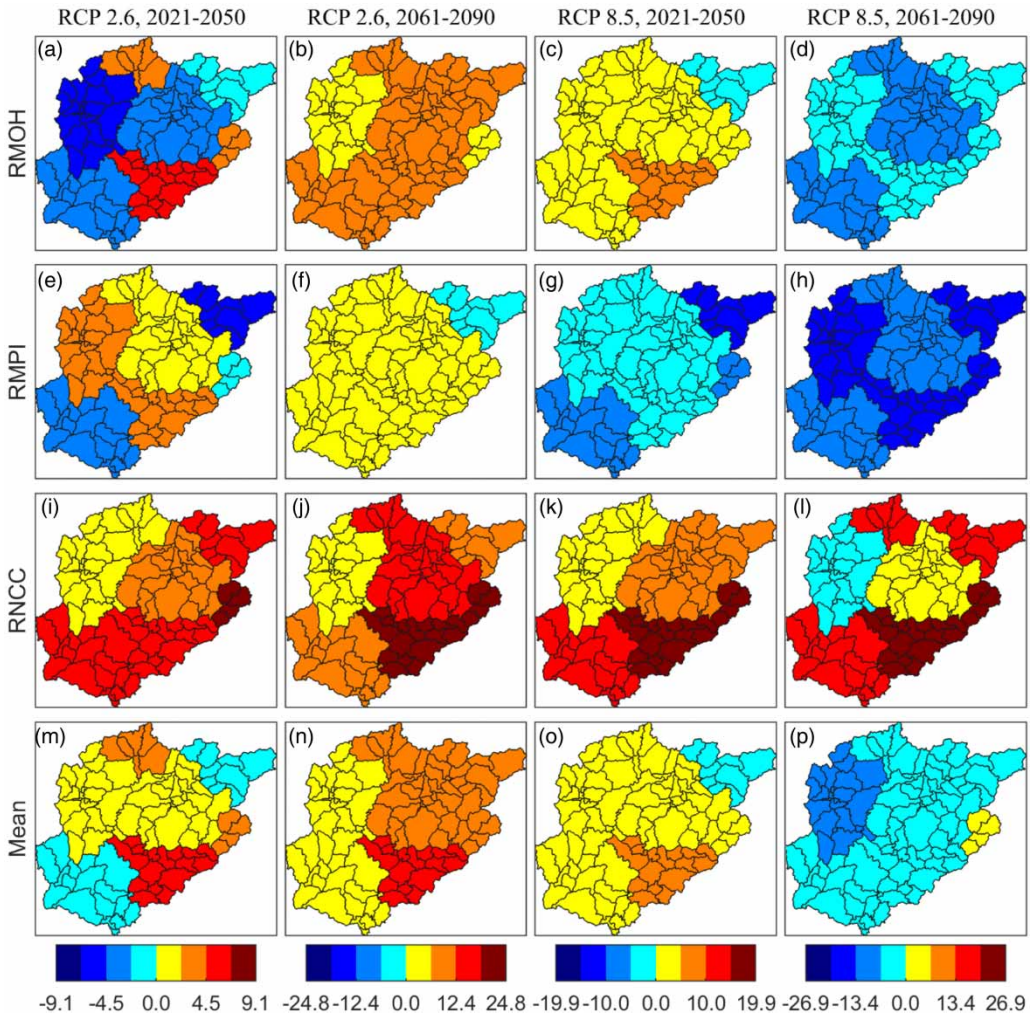

Figure 6 | Relative changes (%) of precipitation under the RCP 2.6 and 8.5 scenarios for the near future period (2021–2050) and far future period (2061–2090) in comparison to the 1970–2005 control period.

RNCC RCP 8.5, most of the sub-basins are suggested to increase considerably in the far future, except for the northeastern areas which is likely to decrease by 9.3%. The ensemble mean of blue water suggests a basin-wide increase under RCP 2.6, with the southeastern portion of the basin expected to have the largest increase of 7.7% in the near future and a continuous increase to 22.5% in the far future. Under RCP 8.5, the blue water in the southern part of the basin is expected to increase by 6.6–13.3% in the near future, while only a slight increase (~5.6%) is suggested in the far future. The blue water in the basin north seems to have only slight increases (~5.3%) in the near future, but they turn to decrease around 2.3–14.2% in the far future. As presented in Figure 5(d), all RCMs suggest that the basin average blue water would continuously increase from near to far future under RCP 2.6, but the changing pattern would be notably different under RCP 8.5. The annual blue water from the RCM mean is expected to increase by 2.8% (29.9 mm) under RCP 2.6 and by 4.8% (51.4 mm) under RCP 8.5 in the near future, benchmarked with the control period. In the long run, the RCM mean suggests that the blue water would experience an increase of 12.4% (134.1 mm) under RCP 2.6 and a slight decrease of 1.7% (18.6 mm) under RCP 8.5. Obviously, the changes of basin-scale averaged blue water and precipitation are in a similar pattern, as blue water is sensitive to the precipitation variability in the Beijiang River basin.

4. DISCUSSION

From this study, it is revealed that the water resources of the Beijiang River basin are dominated by blue water. This somewhat differs from study results for other basins where green water is normally the major player. For instance, in the Hai River basin

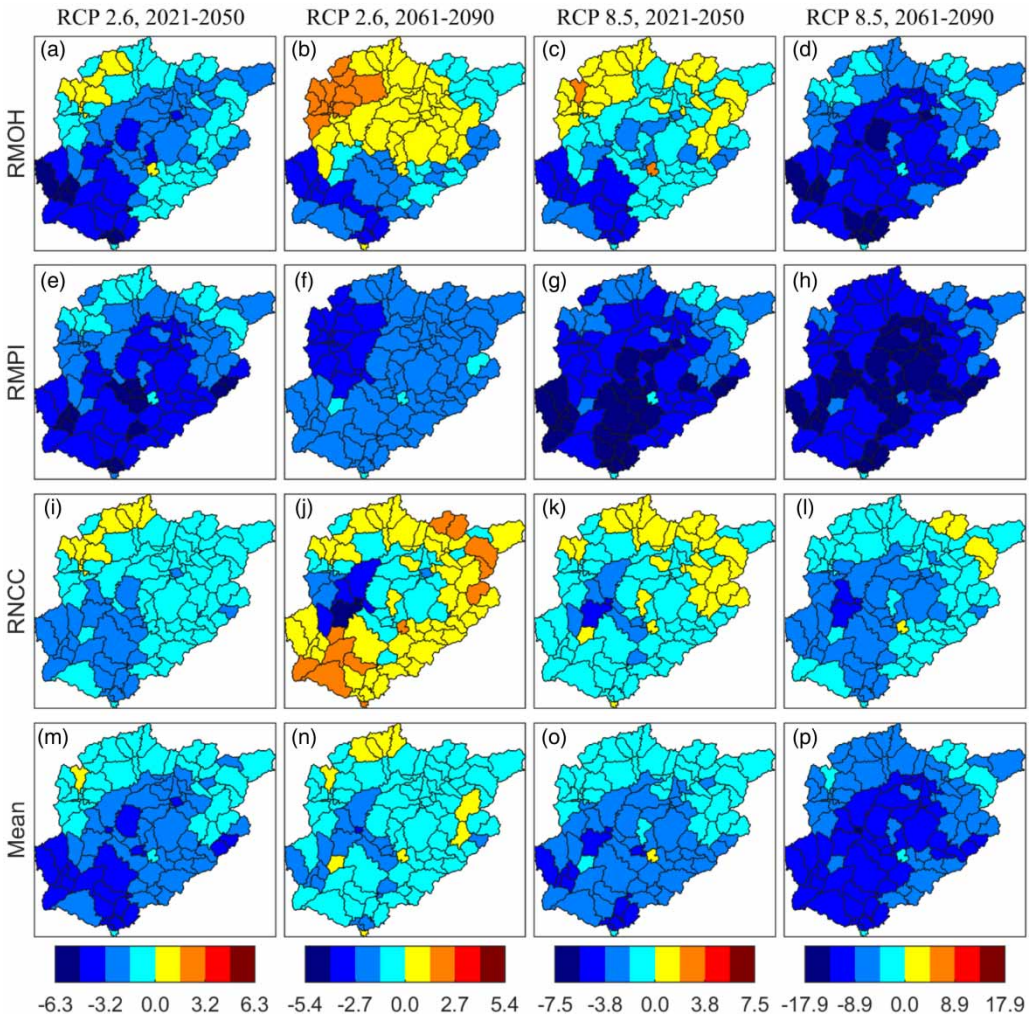

Figure 7 | Same as in Figure 6 but for green water flow.

of northern China, Zhu *et al.* (2018) indicated that the annual mean green water (about 74% of the precipitation) is about 2.8 times higher than the blue water. Faramarzi *et al.* (2009) used SWAT to estimate the water footprint components of 30 provinces in Iran, and indicated that the green water was significantly higher than blue water in more than 20 provinces with annual rainfall being less than 1,100 mm. Schuol *et al.* (2008b) estimated the blue–green water distribution over the hot, low rainfall, dry continent of Africa, and found that the annual average green water amount was significantly more than the blue one in almost all African countries. These mentioned basins are characterized by low rainfall, dryness and intense evapotranspiration, which leads to low levels of surface runoff and high conversion rates of precipitation to green water. The Beijiang River basin is categorized to have the subtropical monsoon climate and its high precipitation (~1,800 mm) tends to meet plant retention, infiltration, puddle filling losses and saturated soil layers; this has resulted in an extensive surface runoff generation and thus brought a larger amount of blue water in comparison to green. The previous studies on the Dongjiang River basin, which is adjacent to the Beijiang River basin, have given similar findings (Wu & Chen 2013; Lyu *et al.* 2017).

By comparing a number of study cases on the annual changes of water components in the literature (see Supplementary Table S4), it is found that the climate change impact on the water components in the studied basin seems to be less significant. This might be due to variations of different climate prediction models, emission settings, downscaling techniques, basin geographical and climatic characteristics, and future projection timeframes. More importantly, accordingly to the projection of ensemble mean of three RCMs, climate change may pose a small increasing effect on precipitation (<10%) in the Beijiang River basin, but there are still areas in the basin where blue and green water may decrease. It is thus essential to explore

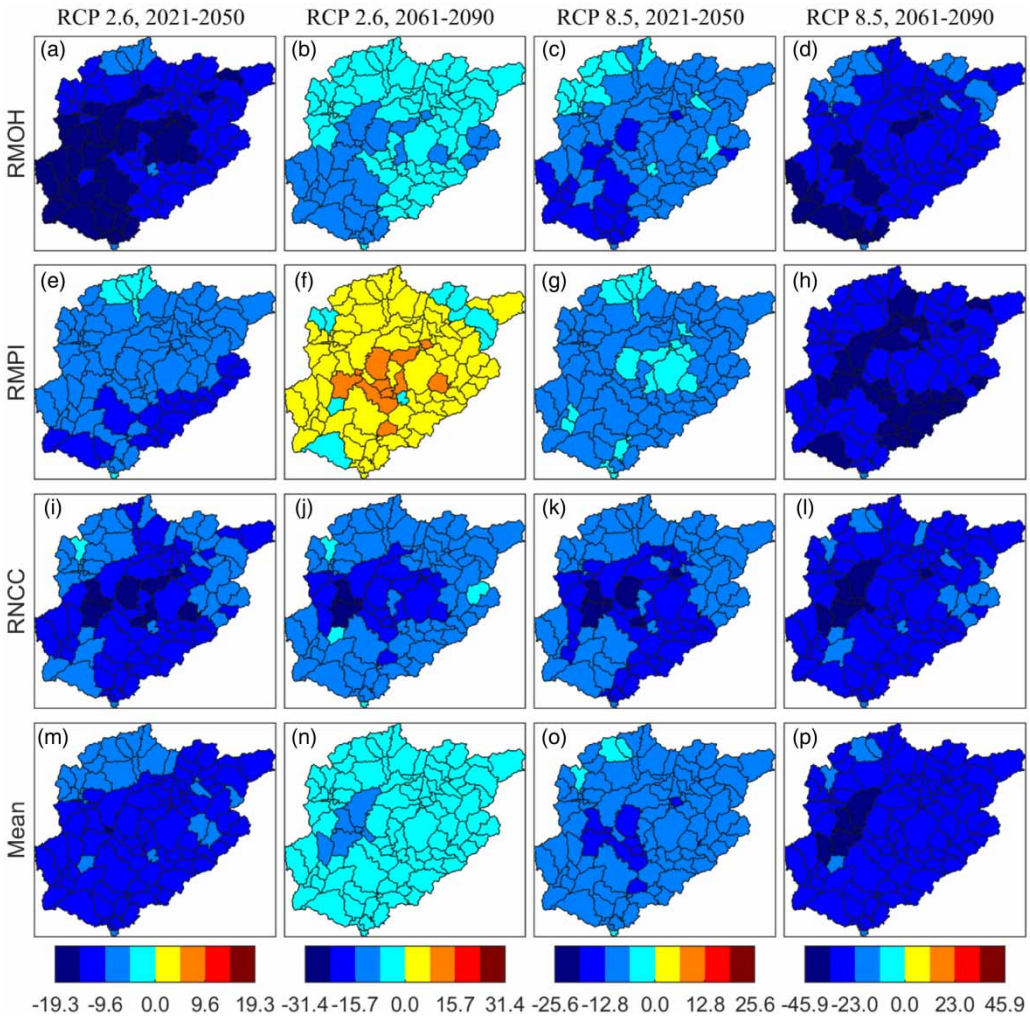

Figure 8 | Same as in Figure 6 but for green water storage.

responsive strategies to reduce adverse influences. For example, creating a contour farming environment by building horizontal terraces or field water storage ditches could enhance the subsurface infiltration rate and soil permeability and increase soil moisture content and green water storage (Srivastava *et al.* 2010). Some farmland management practices (e.g. plastic mulching and intensive cultivation) could mitigate the loss of soil evapotranspiration and reduce inefficient green water flow (Yang *et al.* 2015). Improving irrigation efficiency and seeking optimal allocation of water resources for agricultural, industrial, domestic and ecological uses are also effective strategies for coping with shrinking blue water resources.

To explore whether the RCM with 25 km×25 km resolution is sufficient for evaluating the climatic impact on the studied basin, we used the raw RCM data (i.e. uncorrected RCM) to drive the SWAT to calculate the spatial changes of water components (Supplementary Figures S7–S9). A comparison of Supplementary Figure S7 and Figure 7 shows that the areal green water flow changes remain largely consistent for all scenarios, and the magnitudes of changes are very close between using the uncorrected and corrected RCMs. By comparing Supplementary Figure S8 and Figure 8, it is revealed that the spatial distribution of green water storage changes remains largely consistent, but the magnitude of changes somewhat differs. For example, the western central portion of the basin is expected to experience the largest reduction (~31.4%) in green water storage in the near future based on corrected RNCC RCP 2.6 but the magnitude of such a reduction would be 15.4% based on the uncorrected scenario. A comparison of Supplementary Figure S9 and Figure 9 shows that the areal blue water changes and the relevant ranges demonstrate considerable differences. For example, the increasing trend is projected in the southeast of the basin in the far future based on the uncorrected RMOH RCP 8.5, but such a trend would be reversed under the corrected scenario. Moreover, the southeast portion of the basin would experience the largest increase in blue water (~31.6%) in the

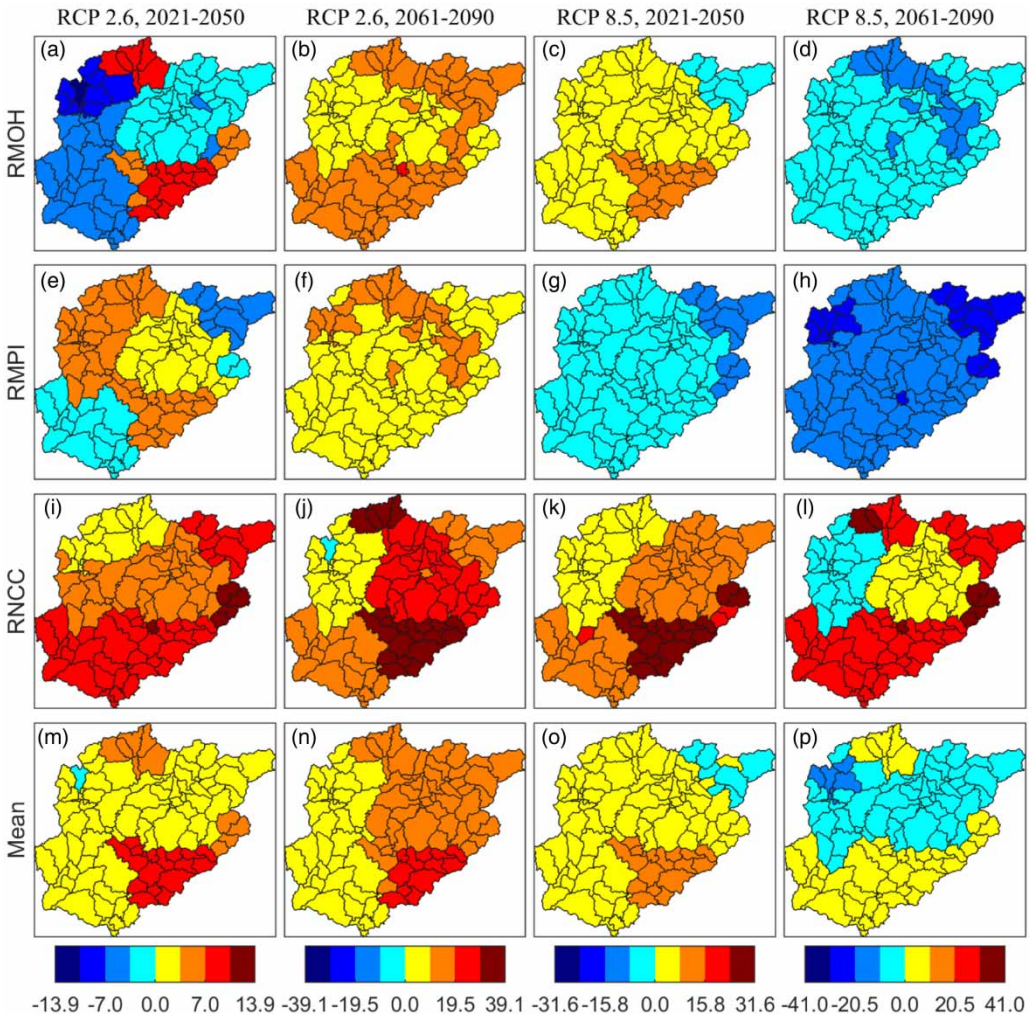

Figure 9 | Same as in Figure 6 but for blue water.

near future based on the corrected RNCC RCP 8.5, but such an increase would rise up to about 54.0% based on the uncorrected scenario. Overall, applying the corrected and uncorrected RCMs to evaluate the climate influences may have notable differences in both the spatial distribution and magnitude of water component changes.

In this work, the blue–green water distribution in the Beijiang River basin was estimated based on the SWAT model. In terms of data, the absence of multi-year land use data and observed evapotranspiration data may somewhat affect calibration, although the performance of the model was still considered satisfactory. In a long run, both land use and climate change are major considerations for water resources management (Pan *et al.* 2017). Land use is mainly associated with evapotranspiration, runoff, infiltration and soil water redistribution, which are indirectly linked to the blue and green water patterns. This study did not address the impact of land use due to insufficient land use data to predict future land use conditions. Moreover, rivers in the basin are likely to be subject to human interventions such as the construction of reservoirs. However, it is rather challenging to obtain the detailed information on the planned reservoirs in the basin in the long term. Thus, the impact of possible planned reservoirs on water resources is not considered in this study. In terms of computation of water components, SWAT only simulates the hydrological cycle without considering their complex interconversions (Zhang *et al.* 2020).

5. CONCLUSION

This study quantitatively evaluated the potential climate change impact on spatiotemporal distributions of blue and green water resources in the Beijiang River basin, southern China. The climate data was based on three CORDEX-EAS RCMs

under RCP 2.6 and 8.5 scenarios for three windows. Then, the hydrometric data was predicted by using the SWAT model which was validated using historical data. The QDM method was adopted to reduce the systematic bias from the original CORDEX-EAS RCMs. From the study, the annual average total water resources over the Beijiang River basin from 1975 to 2004 are 1,741.46 mm, of which 33.3% is green water flow, 2.1 % is green water storage and 64.6% is blue water. The basin's water budget is dominated by blue water, which is about twice as much as green. Spatially, the blue water has an annual mean from 796 to 1,640 mm over the entire basin, and is richly distributed in the central and southeast areas. Green water is relatively higher in the north and lower in both central and southwest areas. The average annual green water storage shows a generally decreasing pattern from north to south.

Compared with the control period, the RCM mean of the average annual precipitation would experience somewhat increases (<10%) in most sub-basins in the near term, but a general decrease under RCP 8.5 in the long run. The largest increase and decrease of green water flow from various RCMs are found to be about 2.7% in the northwestern part of the basin under RMOH RCP 2.6 for 2061–2090 and about 17.9% in the central part of the basin under RMPI RCP 8.5 for 2061–2090, respectively. The basin-wide average of green water flow from three RCM averages is projected to decrease by 43.3 mm under RCP 8.5 in the far future. In addition, the relative reduction of future green water storage projected by RNCC is more than 30% in most of the basin under RCP 8.5 in the far future, whereas the absolute change ranges from 3.8 to 17.4 mm under most scenarios. In terms of blue water, RNCC suggests a significant increase in the southeast portion of the basin under most scenarios in the far future; however, RMPI RCP 8.5 indicates a significant decrease in the northeast portion. In general, the ensemble mean of the three RCMs shows a slight decreasing trend in the north portion of the basin and an increasing one in the south under RCP 8.5 in the far future, and an overall increasing trend in most of the basin under other climate scenarios.

Overall, this study helped gain an insight into the future green and blue water resources in the Beijiang River basin. In light of the global climate change, such information would be useful to policy makers in local water resources management. For example, the shrinkage of blue water implies a decrease of easily available water supply, thus, more efficient irrigation practices and rational water allocation schemes are necessary. In addition, some further improvements are still needed. For example, more observed data (such as evapotranspiration and groundwater flow data) can be utilized to validate SWAT and improve its accuracy in computing blue–green water distributions. Also, the contribution of land use alterations to blue and green water components ought to be investigated in detail. Moreover, only three RCMs were used in this study. As the CORDEX-EAS project develops, more reliable studies of climate change impacts using more RCMs projections can be achieved in the future.

ACKNOWLEDGEMENTS

This work was supported by the National Natural Science Foundation of China (52009022) and AcRF Tier 1 project (2019-T1-001-160) from the Ministry of Education (MOE), Singapore. We gratefully acknowledge the CORDEX-East Asia Databank (https://esgf-data.dkrz.de/search/cordex-dkrz/), which is responsible for the CORDEX dataset. The authors are also thankful for the China Meteorological Data Sharing Service System for providing the observed climate dataset.

DATA AVAILABILITY STATEMENT

All relevant data are included in the paper or its Supplementary Information.

CONFLICTS OF INTEREST

The authors declare there is no conflict.

REFERENCES

Abbaspour, K. C., Yang, J., Maximov, I., Siber, R., Bogner, K., Mieleitner, J., Zobrist, J. & Srinivasan, R. 2007 Modelling hydrology and water quality in the pre-alpine/alpine Thur watershed using SWAT. *Journal of Hydrology* **333**, 413–430.

Afshar, A. A., Hassanzadeh, Y., Pourreza-Bilondi, M. & Ahmadi, A. 2018 Analyzing long-term spatial variability of blue and green water footprints in a semi-arid mountainous basin with MIROC-ESM model (case study: Kashafrood River Basin, Iran). *Theoretical and Applied Climatology* **134**, 885–899.

Arnell, N. W., Hudson, D. & Jones, R. G. 2003 Climate change scenarios from a regional climate model: estimating change in runoff in Southern Africa. *Journal of Geophysical Research: Atmospheres* **108**, 4519.

Arnold, J. G., Srinivasan, R., Muttiah, R. S. & Williams, J. R. 1998 Large area hydrologic modeling and assessment part I: model development. *Journal of the American Water Resources Association* **34**, 73–89.

Badou, D. F., Diekkrüger, B., Kapangaziwiri, E., Mbaye, M. L., Yira, Y., Lawin, E. A., Oyerinde, G. T. & Afouda, A. 2018 Modelling blue and green water availability under climate change in the Beninese Basin of the Niger River Basin, West Africa. *Hydrological Processes* **32**, 2526–2542.

Batjes, N. 1997 A world dataset of derived soil properties by FAO–UNESCO soil unit for global modelling. *Soil Use and Management* **13**, 9–16.

Brown, J. F., Loveland, T. R., Ohlen, D. O. & Zhu, Z. L. 1999 The global land-cover characteristics database: the users' perspective. *Photogrammetric Engineering and Remote Sensing* **65**, 1069–1074.

Cannon, A. J., Sobie, S. R. & Murdock, T. Q. 2015 Bias correction of GCM precipitation by quantile mapping: how well do methods preserve changes in quantiles and extremes? *Journal of Climate* **28**, 6938–6959.

Chakilu, G. G., Sándor, S. & Zoltán, T. 2020 Change in stream flow of Gumara Watershed, upper Blue Nile Basin, Ethiopia under representative concentration pathway climate change scenarios. *Water* **12**, 3046.

Cooper, C. M., Troutman, J. P., Awal, R., Habibi, H. & Fares, A. 2022 Climate change-induced variations in blue and green water usage in US urban agriculture. *Journal of Cleaner Production* **348**, 131326.

Dai, C. & Qin, X. 2019 Assessment of the effectiveness of a multi-site stochastic weather generator on hydrological modelling in the Red Deer River watershed, Canada. *Hydrological Sciences Journal* **64**, 1616–1628.

Dong, N., Yu, Z., Gu, H., Yang, C., Yang, M., Wei, J., Wang, H., Arnault, J., Laux, P. & Kunstmann, H. 2019 Climate-induced hydrological impact mitigated by a high-density reservoir network in the Poyang Lake Basin. *Journal of Hydrology* **579**, 124148.

Falkenmark, M. & Rockström, J. 2006 The new blue and green water paradigm: breaking new ground for water resources planning and management. *Journal of Water Resources Planning and Management* **132**, 129–132.

Faramarzi, M., Abbaspour, K. C., Schulin, R. & Yang, H. 2009 Modelling blue and green water resources availability in Iran. *Hydrological Processes* **23**, 486–501.

Faramarzi, M., Srinivasan, R., Iravani, M., Bladon, K. D., Abbaspour, K. C., Zehnder, A. J. & Goss, G. G. 2015 Setting up a hydrological model of Alberta: data discrimination analyses prior to calibration. *Environmental Modelling & Software* **74**, 48–65.

Farsani, I. F., Farzaneh, M., Besalatpour, A., Salehi, M. & Faramarzi, M. 2019 Assessment of the impact of climate change on spatiotemporal variability of blue and green water resources under CMIP3 and CMIP5 models in a highly mountainous watershed. *Theoretical and Applied Climatology* **136**, 169–184.

Gosling, S., Taylor, R. G., Arnell, N. & Todd, M. 2011 A comparative analysis of projected impacts of climate change on river runoff from global and catchment-scale hydrological models. *Hydrology and Earth System Sciences* **15**, 279–294.

Gu, H., Yu, Z., Yang, C. & Ju, Q. 2018a Projected changes in hydrological extremes in the Yangtze River Basin with an ensemble of regional climate simulations. *Water* **10**, 1279.

Gu, H., Yu, Z., Yang, C., Ju, Q., Yang, T. & Zhang, D. 2018b High-resolution ensemble projections and uncertainty assessment of regional climate change over China in CORDEX East Asia. *Hydrology and Earth System Sciences* **22**, 3087–3103.

Hoegh-Guldberg, O., Jacob, D., Taylor, M., Bolaños, T. G., Bindi, M., Brown, S., Camilloni, I. A., Diedhiou, A., Djalante, R. & Ebi, K. 2019 The human imperative of stabilizing global climate change at 1.5 C. *Science* **365**, eaaw6974.

Hu, H., Yang, K., Sharma, A. & Mehrotra, R. 2020 Assessment of water and energy scarcity, security and sustainability into the future for the Three Gorges Reservoir using an ensemble of RCMs. *Journal of Hydrology* **586**, 124893.

Islam, M., Aramaki, T. & Hanaki, K. 2005 Development and application of an integrated water balance model to study the sensitivity of the Tokyo metropolitan area water availability scenario to climatic changes. *Water Resources Management* **19**, 423–445.

Islam, S., Aramaki, T. & Hanaki, K. 2007 GCM-based analysis of water availability along the Tone River and Tokyo Metropolitan Area under climatic changes. *Regional Environmental Change* **7**, 15–26.

Jacob, D. 2001 A note to the simulation of the annual and inter-annual variability of the water budget over the Baltic Sea drainage basin. *Meteorology and Atmospheric Physics* **77**, 61–73.

Li, M. 2015 *Research on Hydrological Response to Land Cover and Meteorological Factors Change Base on SWAT Model in Beijiang River Basin*. Graduate School of Chinese Academy of Sciences (Guangzhou Institute of Geochemistry).

Li, C., Tang, G. & Hong, Y. 2018 Cross-evaluation of ground-based, multi-satellite and reanalysis precipitation products: applicability of the Triple Collocation method across Mainland China. *Journal of Hydrology* **562**, 71–83.

Lirong, S. & Jianyun, Z. 2012 Hydrological response to climate change in Beijiang River Basin based on the SWAT model. *Procedia Engineering* **28**, 241–245.

Loáiciga, H., Maidment, D. & Valdes, J. 2000 Climate-change impacts in a regional karst aquifer, Texas, USA. *Journal of Hydrology* **227**, 173–194.

Luo, Y., Liu, S., Fu, S., Liu, J., Wang, G. & Zhou, G. 2008 Trends of precipitation in Beijiang River basin, Guangdong province, China. *Hydrological Processes* **22**, 2377–2386.

Lyu, L., Wang, X., Jiang, Y. & Sun, C. 2017 Research on spatial and temporal distribution features of green and blue water in Dongjiang River Basin based on SWAT model. *Water Resources Protection* **33**, 53–60 (in Chinese).

Mishra, S. K. & Singh, V. P. 2004 Long-term hydrological simulation based on the soil conservation service curve number. *Hydrological Processes* **18**, 1291–1313.

Moriasi, D. N., Arnold, J. G., Van Liew, M. W., Bingner, R. L., Harmel, R. D. & Veith, T. L. 2007 Model evaluation guidelines for systematic quantification of accuracy in watershed simulations. *Transactions of the ASABE* **50**, 885–900.

Naderi, M. 2020 Assessment of water security under climate change for the large watershed of Dorudzan Dam in southern Iran. *Hydrogeology Journal* **28**, 1553–1574.

Ngai, S. T., Tangang, F. & Juneng, L. 2017 Bias correction of global and regional simulated daily precipitation and surface mean temperature over Southeast Asia using quantile mapping method. *Global and Planetary Change* **149**, 79–90.

Padhiary, J., Patra, K. C., Dash, S. S. & Uday Kumar, A. 2020 Climate change impact assessment on hydrological fluxes based on ensemble GCM outputs: a case study in eastern Indian River Basin. *Journal of Water and Climate Change* **11**, 1676–1694.

Pan, S., Liu, D., Wang, Z., Zhao, Q., Zou, H., Hou, Y., Liu, P. & Xiong, L. 2017 Runoff responses to climate and land use/cover changes under future scenarios. *Water* **9**, 475.

Pandey, B. K., Gosain, A., Paul, G. & Khare, D. 2017 Climate change impact assessment on hydrology of a small watershed using semi-distributed model. *Applied Water Science* **7**, 2029–2041.

Pandey, B. K., Khare, D., Kawasaki, A. & Mishra, P. K. 2019 Climate change impact assessment on blue and green water by coupling of representative CMIP5 climate models with physical based hydrological model. *Water Resources Management* **33**, 141–158.

Piani, C., Haerter, J. & Coppola, E. 2010 Statistical bias correction for daily precipitation in regional climate models over Europe. *Theoretical and Applied Climatology* **99**, 187–192.

Pietikäinen, J.-P., Markkanen, T., Sieck, K., Jacob, D., Korhonen, J., Räisänen, P., Gao, Y., Ahola, J., Korhonen, H. & Laaksonen, A. 2018 The regional climate model REMO (v2015) coupled with the 1-D freshwater lake model FLake (v1): Fenno-Scandinavian climate and lakes. *Geoscientific Model Development* **11**, 1321–1342.

Rockström, J., Falkenmark, M., Karlberg, L., Hoff, H., Rost, S. & Gerten, D. 2009 Future water availability for global food production: the potential of green water for increasing resilience to global change. *Water Resources Research*. https://doi.org/10.1029/2007WR006767.

Rodrigues, D. B., Gupta, H. V. & Mendiondo, E. M. 2014 A blue/green water-based accounting framework for assessment of water security. *Water Resources Research* **50**, 7187–7205.

Rummukainen, M. 2016 Added value in regional climate modeling. *WIREs Climate Change* **7**, 145–159.

Sahoo, G., Schladow, S., Reuter, J., Coats, R., Dettinger, M., Riverson, J., Wolfe, B. & Costa-Cabral, M. 2013 The response of Lake Tahoe to climate change. *Climatic Change* **116**, 71–95.

Schuol, J., Abbaspour, K. C., Srinivasan, R. & Yang, H. 2008a Estimation of freshwater availability in the West African sub-continent using the SWAT hydrologic model. *Journal of Hydrology* **352**, 30–49.

Schuol, J., Abbaspour, K. C., Yang, H., Srinivasan, R. & Zehnder, A. J. 2008b Modeling blue and green water availability in Africa. *Water Resources Research* **44**, W07406.

Srivastava, R., Sharma, H. & Raina, A. 2010 Suitability of soil and water conservation measures for watershed management using geographical information system. *Journal of Soil and Water Conservation* **9**, 148–153.

Taylor, K. E., Stouffer, R. J. & Meehl, G. A. 2012 An overview of CMIP5 and the experiment design. *Bulletin of the American Meteorological Society* **93**, 485–498.

Teutschbein, C. & Seibert, J. 2012 Bias correction of regional climate model simulations for hydrological climate-change impact studies: review and evaluation of different methods. *Journal of Hydrology* **456**, 12–29.

Tong, Y., Gao, X., Han, Z., Xu, Y., Xu, Y. & Giorgi, F. 2021 Bias correction of temperature and precipitation over China for RCM simulations using the QM and QDM methods. *Climate Dynamics* **57**, 1425–1443.

Touseef, M., Chen, L., Masud, T., Khan, A., Yang, K., Shahzad, A., Ijaz, M. W. & Wang, Y. 2020 Assessment of the future climate change projections on streamflow hydrology and water availability over Upper Xijiang River Basin, China. *Applied Sciences* **10**, 3671.

Trajkovic, S. 2007 Hargreaves versus Penman-Monteith under humid conditions. *Journal of Irrigation and Drainage Engineering* **133**, 38–42.

Veettil, A. V. & Mishra, A. K. 2016 Water security assessment using blue and green water footprint concepts. *Journal of Hydrology* **542**, 589–602.

Volosciuk, C., Maraun, D., Vrac, M. & Widmann, M. 2017 A combined statistical bias correction and stochastic downscaling method for precipitation. *Hydrology and Earth System Sciences* **21**, 1693–1719.

Wilcke, R. A. I., Mendlik, T. & Gobiet, A. 2013 Multi-variable error correction of regional climate models. *Climatic Change* **120**, 871–887.

Wu, Y. & Chen, J. 2013 Analyzing the water budget and hydrological characteristics and responses to land use in a monsoonal climate river basin in South China. *Environmental Management* **51**, 1174–1186.

Wu, C., Huang, G. & Yu, H. 2015 Prediction of extreme floods based on CMIP5 climate models: a case study in the Beijiang River basin, South China. *Hydrology & Earth System Sciences* **19**, 1385–1399.

Yang, N., Sun, Z. X., Feng, L. S., Zheng, M. Z., Chi, D. C., Meng, W. Z., Hou, Z. Y., Bai, W. & Li, K. Y. 2015 Plastic film mulching for water-efficient agricultural applications and degradable films materials development research. *Materials and Manufacturing Processes* **30**, 143–154.

Yuan, Z., Xu, J., Meng, X., Wang, Y., Yan, B. & Hong, X. 2019a Impact of climate variability on blue and green water flows in the Erhai Lake Basin of Southwest China. *Water* **11**, 424.

Yuan, Z., Xu, J. & Wang, Y. 2019b Historical and future changes of blue water and green water resources in the Yangtze River source region, China. *Theoretical and Applied Climatology* **138**, 1035–1047.

Zhang, Y., Tang, C., Ye, A., Zheng, T., Nie, X., Tu, A., Zhu, H. & Zhang, S. 2020 Impacts of climate and land-use change on blue and green water: a case study of the Upper Ganjiang River Basin, China. *Water* **12**, 2661.

Zhang, D. J., Lin, Q. Y., Yao, H. X., He, Y. R., Deng, J. & Zhang, X. X. 2021 Accelerating SWAT simulations using an in-memory NoSQL database. *Journal of Environmental Informatics* **37**, 142–152.

Zhao, A., Zhu, X., Liu, X., Pan, Y. & Zuo, D 2016 Impacts of land use change and climate variability on green and blue water resources in the Weihe River Basin of northwest China. *Catena* **137**, 318–327.

Zhu, K., Xie, Z., Zhao, Y., Lu, F., Song, X., Li, L. & Song, X. 2018 The assessment of green water based on the SWAT model: a case study in the Hai River Basin, China. *Water* **10**, 798.

Zuo, D., Xu, Z., Peng, D., Song, J., Cheng, L., Wei, S., Abbaspour, K. C. & Yang, H. 2015 Simulating spatiotemporal variability of blue and green water resources availability with uncertainty analysis. *Hydrological Processes* **29**, 1942–1955.

First received 2 March 2022; accepted in revised form 24 June 2022. Available online 5 July 2022